

to increase as  $z_0$  decreases) and that  $\sigma \ll \delta\omega_0$ . Thus, if  $\alpha$  and  $\beta$  are comparable in magnitude, the condition  $\beta\delta\omega_0 z_0 \tau \gg 1$  is mandatory for enhancement. For example, if  $\eta\tau \ll 1$  and  $\omega_p t_2 \gg 1$ , we have  $\beta = 2\alpha$ . For simplicity we assume  $\alpha z_0 \sigma \tau$ ,  $\beta z_0 \sigma \tau > \sqrt{2}$  so that one exponential dominates and the oscillations are negligible. The result is then Eq. (12).

Note that the observed rate of echo decay contains  $\eta$  through the parameters  $\lambda_0$ ,  $\lambda_1$ ,  $\lambda_2$ , and  $\beta$ . Depending on the relative sizes of  $\lambda_0$ ,  $\lambda_1$ , and  $\lambda_2$ , the characteristic decay rate for the echo amplitude is between  $\frac{1}{2}\eta + T^{-1}$  and  $\frac{3}{2}\eta + T^{-1}$ .

#### APPENDIX B: ECHO FOR $t_3 < \tau$

Equation (A1) still holds in this case (with a modified  $a_{mn}$ ), but  $\Delta\omega_{2i}$  is given by the more complex Eq. (14) rather than Eq. (8) which neglects initial transverse magnetization. The same arguments

which lead from Eq. (A1) to (A2) and (A3) should now be multiplied by  $J_0(\delta\omega_i a) J_0(\delta\omega_i b) J_0(\delta\omega_i c)$  and other combinations of three Bessel functions resulting from Fourier components that do not contain the phase  $\Delta\omega_{0i} t_3$ .

There are competing effects in the initial transverse components  $x_0$ ,  $y_0$  which tend to cause an increase in echo amplitude. These arise from terms of the form

$$y_0 e^{i(\Delta\omega_i \pm \Delta\omega_2)\tau}$$

which can have a dc component as a result of Eq. (14). Such dc components, however, require products of four Bessel functions, at least one of which must be of nonzero order. Because of this, we assume these terms to be small compared with the previously mentioned ones which cause a decrease in echo amplitude.

<sup>1</sup>C. R. Christensen, B. D. Guenther, and A. C. Daniel, Bull. Am. Phys. Soc. **14**, 1185 (1969).

<sup>2</sup>D. E. Kaplan, R. M. Hill, and G. F. Herrmann, Phys. Rev. Letters **20**, 1156 (1968).

<sup>3</sup>R. S. Harp and R. R. Smith, Phys. Letters **29A**, 317 (1969).

<sup>4</sup>R. W. Gould, Phys. Letters **29A**, 347 (1969).

<sup>5</sup>G. F. Herrmann, D. E. Kaplan, and R. M. Hill, Phys. Rev. **181**, 829 (1969).

<sup>6</sup>R. M. Hill, D. E. Kaplan, G. F. Herrmann, and S. K. Ichiki, J. Appl. Phys. **41**, 929 (1970).

<sup>7</sup>B. D. Guenther, C. R. Christensen, and A. C. Daniel, Phys. Letters **30A**, 391 (1969).

<sup>8</sup>P. G. De Gennes, P. A. Pincus, F. Hartmann-Boutron, and J. M. Winter, Phys. Rev. **129**, 1105 (1963).

<sup>9</sup>E. L. Hahn, Phys. Rev. **80**, 580 (1950).

<sup>10</sup>I. D. Abella, N. A. Kurnit, and S. R. Hartmann, Phys. Rev. **141**, 391 (1966).

<sup>11</sup>W. H. Kegel and R. W. Gould, Phys. Letters **19**, 531 (1965).

<sup>12</sup>G. F. Herrmann, R. M. Hill, and D. E. Kaplan, Phys. Rev. **156**, 118 (1967); G. F. Herrmann and R. F.

Whitmer, *ibid.* **143**, 122 (1966).

<sup>13</sup>R. Weber and M. H. Seavey, Solid State Commun. **7**, 619 (1969).

<sup>14</sup>B. D. Guenther, C. R. Christensen, A. C. Daniel, and Peter M. Richards, Phys. Letters **33A**, 355 (1970).

<sup>15</sup>Peter M. Richards, Phys. Rev. **173**, 581 (1968).

<sup>16</sup>H. Suhl, Phys. Rev. **109**, 606 (1958); T. Nakamura, Progr. Theoret. Phys. (Kyoto) **20**, 542 (1958).

<sup>17</sup>L. B. Welsh, Phys. Rev. **156**, 370 (1967).

<sup>18</sup>R. J. Mahler and L. W. James, Bull. Am. Phys. Soc. **12**, 1117 (1967).

<sup>19</sup>H. S. Bennett and P. C. Martin, Phys. Rev. **138**, A608 (1965).

<sup>20</sup>D. G. McFadden and R. A. Tahir-Kheli, Phys. Rev. **B 1**, 3649 (1970).

<sup>21</sup>M. E. Lines and E. D. Jones, Phys. Rev. **139**, A1313 (1965).

<sup>22</sup>G. L. Witt and A. M. Portis, Phys. Rev. **136**, A1316 (1964).

<sup>23</sup>G. N. Watson, *A Treatise on the Theory of Bessel Functions* (Cambridge U. P., New York, 1962).

## Direction of the Magnetic Easy Axis in $\gamma'$ -Fe<sub>4</sub>N

J. C. Wood, Jr.\* and A. J. Nozik

American Cyanamid Company, Central Research Division, Stamford, Connecticut 06904

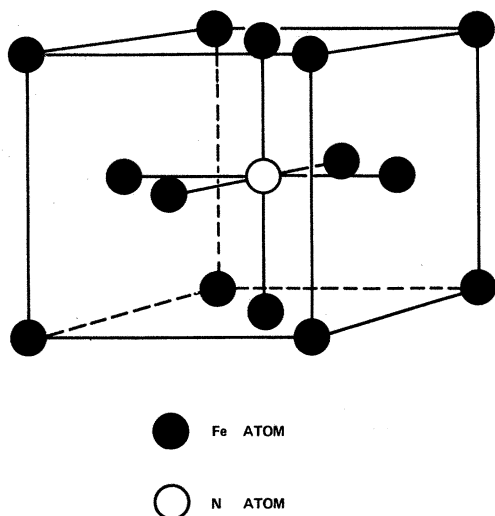
(Received 13 May 1971)

The direction of the easy axis of magnetization in  $\gamma'$ -Fe<sub>4</sub>N has been determined by detailed analysis of certain peaks in the Mössbauer spectrum of a powdered sample in an applied magnetic field. The analysis indicates the magnetic-easy-axis direction to be along  $\langle 100 \rangle$ . The electric field gradient at the face-centered Fe atoms is calculated to be  $-7.0 \times 10^{14}$  esu/cm<sup>3</sup>.

### I. INTRODUCTION

Recent Mössbauer-effect studies<sup>1,2</sup> of  $\gamma'$ -Fe<sub>4</sub>N have shown the existence of two magnetic hyper-

fine patterns for the crystallographically equivalent face-centered iron atoms. These patterns arise because of a difference in the angles between the internal magnetic field and the principal axis of

FIG. 1. Structure of  $\gamma'$ -Fe<sub>4</sub>N.

the electric field gradient (EFG) at these iron sites. We have used this difference in the angles to determine the direction of the magnetic easy axis of  $\gamma'$ -Fe<sub>4</sub>N, employing a randomly oriented powder sample. Normally the easy axis is found by measuring the magnetic anisotropy of single crystals. However, thermodynamic characteristics<sup>3-5</sup> make it difficult to grow single crystals of  $\gamma'$ -Fe<sub>4</sub>N large enough for the determination of magnetic anisotropy.

## II. METHOD OF ANALYSIS

The structure of  $\gamma'$ -Fe<sub>4</sub>N is perovskite<sup>6</sup> (Fig. 1), with the corner iron atoms (Fe I) having local cubic symmetry and the face-centered iron atoms (Fe II) having local axial symmetry. For this structure, the principal axis of the EFG tensor at the Fe II sites should be directed parallel to the line between the nitrogen and the Fe II atoms (i. e., parallel to the crystal axes). For an internal magnetic field  $H$  forming an angle  $\theta$  with the EFG principal axis, the energy levels of the excited nuclear state are given by<sup>7</sup>

$$E = -g\mu_N H m_I + (-1)^{|m_I|+1/2} \frac{e^2 q Q}{8} (3 \cos^2 \theta - 1). \quad (1)$$

The quadrupole splitting ( $S_Q$ ) for this case is then defined as

$$S_Q = \left( \frac{1}{2} e^2 q Q \right) \left( \frac{3 \cos^2 \theta - 1}{2} \right). \quad (2)$$

Thus, for the three Fe II atoms in a unit cell more than one Mössbauer hyperfine pattern would be observed for an arbitrarily directed internal magnetic field. If the internal magnetic field is confined to the  $\{110\}$  plane, two magnetic hyperfine patterns would be observed for all directions except

$\langle 111 \rangle$ . Furthermore, these patterns would have an intensity ratio of 2 : 1 and a  $S_Q$  ratio of -1 : 2. It can be shown that only if the internal field is confined to the  $\{110\}$  plane can two hyperfine patterns with these ratios be obtained. This condition arises strictly from the values of  $(3 \cos^2 \theta - 1)$  that can be assigned to the three Fe II atoms. The EFG ( $eq$ ) at each Fe II site is equal because the sites are crystallographically equivalent. If the internal magnetic field were directed along  $\langle 111 \rangle$ , then only one hyperfine pattern would be observed since  $\theta$  has the same value for all three Fe II atoms.

Our previous data<sup>1,2</sup> showed that the Mössbauer spectrum of  $\gamma'$ -Fe<sub>4</sub>N consisted of two Fe II magnetic hyperfine patterns (Fe II-A and Fe II-B) with an intensity ratio of 2 : 1 and a  $S_Q$  ratio of -1 : 2 (see Fig. 1 and Table I). Thus, the easy axis of  $\gamma'$ -Fe<sub>4</sub>N is in the  $\{110\}$  plane, with the  $\langle 111 \rangle$  direction excluded. Further symmetry considerations dictate that the easy-axis direction is either parallel to  $\langle 100 \rangle$  or  $\langle 110 \rangle$ . However, because the sign of the EFG is not known, unique determination of the easy-axis direction cannot be made from the previous data.

By applying a strong magnetic field to randomly oriented particles the internal magnetic field will become unidirectional in space, but randomly oriented with respect to the crystal axes. Thus, instead of the two  $\theta$  values ( $\theta_A$  and  $\theta_B$ ) which are present in zero field, all values of  $\theta$  from 0 to  $\pi/2$  will be represented by a  $\sin\theta$  distribution. The externally applied field would thus broaden the Mössbauer spectrum and produce changes in peak shape and width which depend upon both the direction of the easy axis and the experimental linewidth ( $\Gamma$ ) in zero field. Hence, a detailed analysis of the powder spectrum in a magnetic field can yield the easy axis of magnetization.

## III. EXPERIMENTAL

The  $\gamma'$ -Fe<sub>4</sub>N was synthesized by reducing iron oxide at 750 °C in a hydrogen atmosphere, followed by nitriding in a hydrogen-ammonia atmosphere at 500 °C. The material was ground, and the small particle  $\gamma'$ -Fe<sub>4</sub>N was randomly incorporated into cured polyester resin to prevent particle rotation in the applied magnetic field. The magnetic field was obtained from a 5-kOe permanent magnet which

TABLE I. Mössbauer parameters of the Fe species in  $\gamma'$ -Fe<sub>4</sub>N.

	$H$ (kG)	Quadrupole splitting (mm/sec)	Isomer shift <sup>a</sup> (mm/sec)	Relative intensity
Fe I	340.6	0.0	+0.24	1.0
Fe II-A	215.5	+0.22	+0.30	2.0
Fe II-B	219.2	-0.43	+0.32	1.0

<sup>a</sup>With respect to Fe metal.

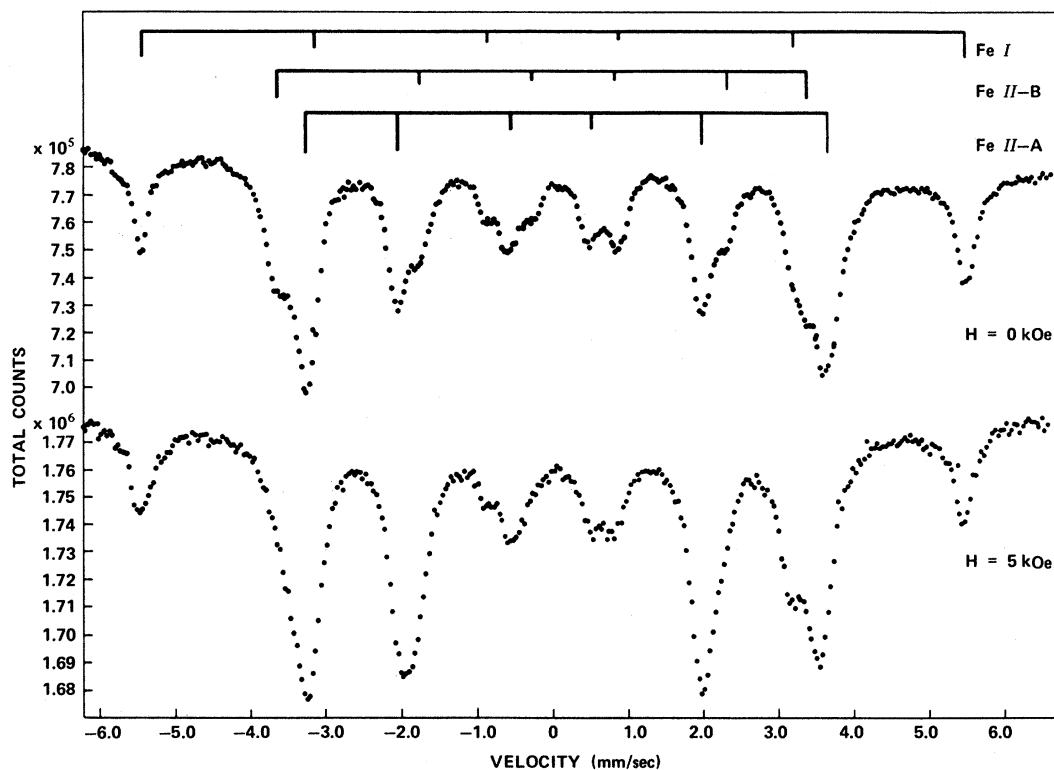


FIG. 2. Mössbauer spectra of  $\gamma'$ -Fe<sub>4</sub>N in zero field and in a 5-kOe field. Line positions indicated at top refer only to the zero-field spectrum.

was positioned so that the direction of the Mössbauer  $\gamma$  rays were perpendicular to the applied field. The Mössbauer source was Co<sup>57</sup> in copper.

#### IV. RESULTS AND DISCUSSION

The Mössbauer spectra obtained at room temperature both with and without an applied magnetic field are shown in Fig. 2. In the zero-field spectrum, the ratio of the integrated intensities for the Fe II-A and Fe II-B sites is 2:1 and the ratio of the  $S_Q$  values is -1:2. In an applied magnetic field the distinction between the Fe II-A and Fe II-B patterns is removed. Also seen in the spectrum is the expected increase in the relative intensity of the second and fifth lines of the magnetic hyperfine pattern due to the alignment of the internal magnetic field perpendicular to the incident  $\gamma$  rays. For perfect alignment the intensity ratios would be 3:4:1:1:4:3. Our spectrum shows intensity ratios of 3:3.8:1:1:3.8:3. These values, along with magnetization measurements in an equivalent magnetic field, indicate that the sample was 98% saturated.

For the analysis of the spectrum we will concentrate on an absorption peak composed solely of absorption lines arising from the Fe II-A and Fe II-B patterns. As seen in Fig. 2, two such peaks exist at about -2 and +2 mm/sec. We will perform

the analysis using data from the peak at -2 mm/sec. We note for this peak that the experimental linewidth  $\Gamma$  of each composite line is approximately equal to the separation  $\Delta$  between them. If we let  $d = 3 \cos^2 \theta - 1$ , then we have

$$\Gamma \sim \Delta = \frac{1}{8} e^2 q Q (d_A - d_B). \quad (3)$$

The values of  $d_A$  and  $d_B$  depend upon the direction of the easy axis of magnetization. For the two possible directions in  $\gamma'$ -Fe<sub>4</sub>N we have the following values:

	$d_A$	$d_B$
$H \parallel \langle 100 \rangle$	-1	2
$H \parallel \langle 110 \rangle$	0.5	-1

With the application of a strong magnetic field,  $d$  assumes all values between -1 and 2 regardless of the direction of the easy axis. The resultant Mössbauer peak is the superposition of a continuous distribution of lines. The actual peak position and shape is obtained by integrating over all possible values of  $d$  weighted with a  $\sin \theta$  distribution function. Figure 3 shows the calculated peak shapes and positions for  $H \parallel \langle 100 \rangle$  and  $\langle 110 \rangle$  both with and without an applied magnetic field. The line position for zero  $S_Q$  is also indicated in the figure. We see that  $H \parallel \langle 100 \rangle$  yields a maximum absorption

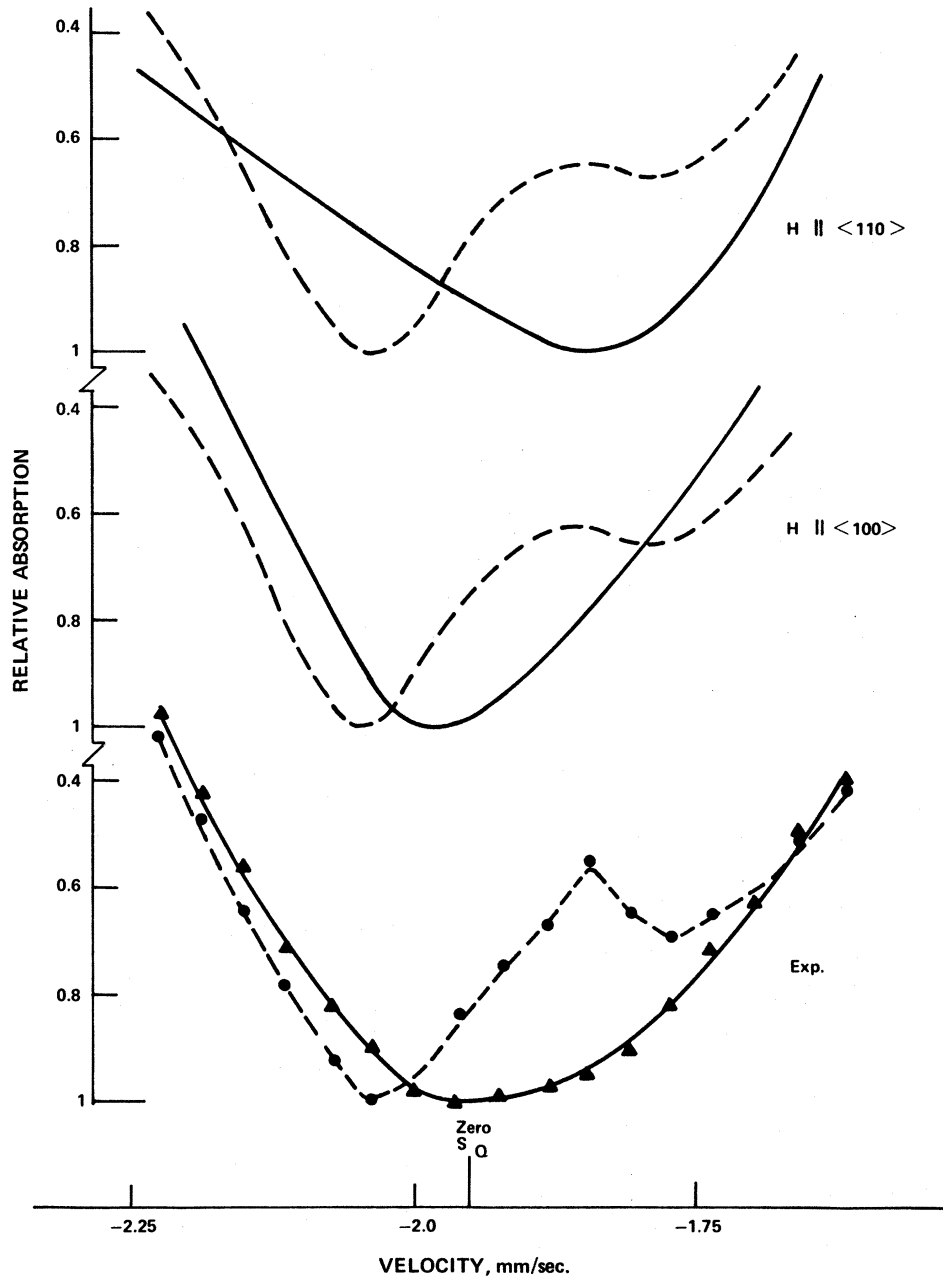


FIG. 3. Shape and position of the Mössbauer peak of  $\gamma'$ -Fe<sub>4</sub>N located at  $-2$  mm/sec. Bottom spectrum shows the experimental peak in zero field (dashed line) and in 5-kOe field (solid line). The top two spectra show the theoretically calculated peaks in zero field (dashed lines) and in 5-kOe field (solid line) for the two possible orientations of the internal magnetic field. The position of the Mössbauer peak calculated for the hypothetical case of zero quadrupole interaction for Fe II is indicated on the abscissa.

which is more negative than the zero  $S_Q$  position, while  $H_{\parallel} \langle 110 \rangle$  gives a maximum absorption less negative than the zero  $S_Q$  position. The skewness of the peak calculated for  $H_{\parallel} \langle 100 \rangle$  is toward the right, and for  $H_{\parallel} \langle 110 \rangle$  the skewness is toward the left. Also the "linewidth" of the peak calculated with  $H_{\parallel} \langle 100 \rangle$  is narrower than the zero-field "linewidth," while the reverse is true for the peak cal-

culated with  $H_{\parallel} \langle 100 \rangle$ . The "linewidths" can also be compared by comparing the full width at half-maximum  $\Gamma_e$  of the peak in an applied magnetic field to the sum of the experimental linewidth and line separation in zero field. We find that

$$\Gamma_e / (\Gamma + \Delta) = 0.68, \quad H_{\parallel} \langle 100 \rangle$$

$$\Gamma_e / (\Gamma + \Delta) = 1.0, \quad H_{\parallel} \langle 110 \rangle.$$

The experimental peak in Fig. 3 shows all the characteristics described above for  $H \parallel \langle 100 \rangle$  and, furthermore,

$$\Gamma_e/(\Gamma + \Delta) = 0.67.$$

Thus, we conclude that the magnetic easy axis in  $\gamma'$ -Fe<sub>4</sub>N lies along the  $\langle 100 \rangle$  direction.

Knowing that the easy axis is along  $\langle 100 \rangle$ , it is

possible to calculate the EFG at the Fe II sites in  $\gamma'$ -Fe<sub>4</sub>N. From Eq. (2), using the  $S_Q$  values in Table I, we find that for the Fe II atoms

$$e^2qQ = -0.87 \text{ mm/sec.} \quad (4)$$

Using the known value of  $Q = +0.2b$ ,<sup>8</sup> we calculate

$$eq = -7.0 \times 10^{14} \text{ esu/cm}^3. \quad (5)$$

\*Present address: TRW, IRC Philadelphia Division, Philadelphia, Pa.

<sup>1</sup>A. J. Nozik, J. C. Wood, Jr., and G. Haacke, *Solid State Commun.* **7**, 1677 (1969).

<sup>2</sup>A. J. Nozik, J. C. Wood, Jr., and G. Haacke, *Solid State Commun.* **8**, viii(E) (1970).

<sup>3</sup>E. Lehrer, *Z. Elektrochem.* **37**, 460 (1930).

<sup>4</sup>P. H. Emmett, S. B. Hendricks, and S. Brunauer, *J. Am. Chem. Soc.* **52**, 1456 (1930).

<sup>5</sup>V. G. Paranjpe, M. Cohen, M. B. Bever, and C. F. Floe, *J. Metals* **188**, 261 (1950).

<sup>6</sup>R. H. Jack, *Proc. Roy. Soc. (London)* **A195**, 34 (1948).

<sup>7</sup>G. K. Wertheim, *Mössbauer Effect: Principles and Applications* (Academic, New York, 1964), p. 82.

<sup>8</sup>A. J. Nozik and M. Kaplan, *Phys. Rev.* **159**, 273 (1967).

PHYSICAL REVIEW B

VOLUME 4, NUMBER 7

1 OCTOBER 1971

## Susceptibility of the $s$ - $d$ Model

K. D. Schotte\*

*Service de Physique Théorique CEA-BP No. 2, Gif-sur-Yvette 91, Saclay, France*

and

U. Schotte

*Institut für Theoretische Physik der Universität Düsseldorf, 4 Düsseldorf, Germany*

(Received 19 April 1971)

The analogy between the thermodynamics of the  $s$ - $d$  model and those of a one-dimensional classical Coulomb gas is exploited to calculate the impurity-spin susceptibility on the computer. The numerical method is a special Monte Carlo procedure first used by Metropolis *et al.* We find a Curie-Weiss form for the static susceptibility with a Néel temperature of about one-third of the Kondo temperature. We discuss the connection between our results and a recent scaling theory of Anderson, Yuval, and Hamann.

### I. INTRODUCTION

In this paper we follow a recent development started by Anderson and Yuval.<sup>1</sup> This theory deals with the fluctuation behavior of the impurity spin. The essential result—and our starting point—is an expression for the partition function for the Kondo or  $s$ - $d$  model<sup>2,3</sup> which turns out to be at the same time the grand partition function of a classical Coulomb gas. The charged particles correspond to spin-up and spin-down flips.

Although this result is not explicit with respect to the physical properties of the  $s$ - $d$  model, one can study the thermodynamics and the correlation functions of the classical gas. Thereby one obtains information about the dynamics of the spin fluctuations and, for example, the susceptibility of the impurity spin.

The static magnetic susceptibility of dilute magnetic alloys has been the subject of intensive theoretical investigations; the results, however, have remained controversial.<sup>4-6</sup> While at high tempera-

tures a Curie-like dependence characterizes the paramagnetic behavior of the impurities, at low temperatures a degradation to less than Curie dependence seems to be the general result of the calculations based on the  $s$ - $d$  model for antiferromagnetic coupling. The current theories differ in the degree of this degradation.

The experimental situation too is not very clear.<sup>7</sup> Qualitatively the behavior described above has been observed on a wide range of dilute alloy systems. However, even for comparatively low concentrations, interaction effects seem to be present<sup>8</sup> and complicate the interpretation. Recent experiments where proper attention to this difficulty has been paid confirm the Curie-Weiss behavior above and near  $T_K$  (for CuMn with  $\Theta = 10$  mK), while far below  $T_K$  a constant plus quadratic term have been measured (for AuV with  $\Theta = 300$  K).<sup>9</sup>

The problem is how to explain the “disappearance” of the spin towards  $T=0$ . Essentially two views have been suggested of the low-temperature be-